Available online at www.sciencedirect.com

ScienceDirect

Energy Procedia 50 (2014) 30 – 40

Energy Procedia

Investigation of the monocrystalline silicon solar cell physical behavior after thermal stress by AC Impedance Spectra

K. Al Abdullah[a], Faisal Al Alloush[b], C. Salame[c]

[a]*Laboratory of microelectronic-University of Aleppo, Faculty of Electrical and electronic Engineering-Aleppo-Syria**
[b]*Postgraduate Student (PhD), University of Aleppo, Faculty of Electrical and electronic Engineering-Aleppo-Syria*
[d]*CNRSL, National Council for Scientific Research, Beirut, Lebanon-LPA, Faculty of Sciences II, Lebanese University, B.P 90656 Jdeidet El Mten, Lebanon*

Abstract

In this work, the DC measurements and AC measurements (impedance spectra) have been used to characterize the mono crystalline silicon solar cell (MSiSC). From the I-V characteristics under dark conditions for different temperatures (298-353K°) and by using the ARRHENIUS diagrams defined by $Ln(I)=f(1/T)|_{v=const}$, we have obtained the barrier height Ψ (eV), ideal factor A, and the reverse saturation current I_0 (A); using the double exponential model.

The AC measurement impedance [X(ω)=f(R(ω))] has been employed to measure the parameters of the MSiSC such as: heterogeneity factor, β, DC resistance R_{dc}, the bulk resistance R_b, activation energy E (eV), donor density N_d (cm^{-3}) and density states N_s (cm^{-2}). The solar cell was exposed to thermal stress within the range (298-353K°), the diagram of complex impedance in the dark, was obtained. This plot give a semicircles arcs, their centers lie below the real axis R(ω), corresponding to the appearance of the depression angle (θ≠0) which allows to measure the heterogeneity factor, β (β=2θ/π) which is in good agreement with the Cole-Cole diagram. It is noted that, β, increases with temperature. The intersection of the circle arcs from the right with x axis (i.e. at very low frequency) gives R_{dc}, while the intersection from the left gives R_b, of the sample (i.e. at very high frequency).

By using ARRHENIUS diagrams defined by Ln(c)=f(1/T) and Ln(f)=f(1/T), we have obtained the parameters E (eV), N_d (cm^{-3}), and Ns (cm^{-2}).

Selection and peer-review under responsibility of the Euro-Mediterranean Institute for Sustainable Development (EUMISD)

Keywords: monocrystalline silicon solar cell, Impedance spectroscopy, Barrier height, heterogeneity factor, DC resistance, bulk resistance, Activation energy, Donor density, Density states;

1. Introduction

Because of the increasing demand for energy and the limited supply of fossil fuels, the search for alternative sources of power is imperative. Given that there is a vast amount of energy available from the sun; devices that convert light energy into electrical energy are becoming increasingly important. Solar or photovoltaic (PV) cells convert light energy into useful electrical power. These cells are produced from light-absorbing materials. When the cell is illuminated, optically generated carriers produce an electric current when the cell is connected to a load [1].

Generally, the operating voltage of an array is fixed and, as the temperature of the array changes the operating point I-V shifts [2]. If a partial shadow is cast on the panel, the shadowed cells are reverse biased by the illuminated cells. A mismatch due to changes of the complex impedance can lead to a reduced performance of the whole power generating system. Hence, for designing such efficient high power photovoltaic systems a detailed study on AC parameters of solar cells is important. In terrestrial applications, the solar cell is exposed to temperatures varying from 10 C° to 50 C° [3].

Impedance spectroscopy is a very powerful technique for solar cell characterization. We have employed this technique in the study of high performance MSiSC, relating the impedance pattern obtained

* Corresponding author. Tel: +963-932 810 820, +963-933404400
E-mail address: m-nasr.al-abdullah@lapost.net, f.alloush@hotmail.com

Selection and peer-review under responsibility of the Euro-Mediterranean Institute for Sustainable Development (EUMISD)
doi:10.1016/j.egypro.2014.06.004

with the theory of the impedance of electron diffusion and recombination in a semiconductor layer. Different cell parameters, as series and parallel resistances, capacitance, diode factor, minority carrier lifetime, acceptor impurities density and depletion layer charge density have been obtained as function of applied bias for different light illumination intensities. The behaviour of cell capacitance under illumination is determined by the applied bias rather than by the light carrier generation when measurement at fixed bias are carried out.

Impedance spectroscopy is particularly characterized by the measurement and analysis of some or all impedance related functions. In impedance spectroscopy, the complex impedance $Z(\omega)=R(\omega)+jX(\omega)$ of a device is measured directly in a large range of frequency [4] Where $R(\omega)$ and $X(\omega)$ are, respectively, the real and imaginary parts of $Z(\omega)$. A purely sinusoidal voltage with different frequencies is applied to the device under test and the phase shift and amplitude of the voltage and current are measured. The ratio between the applied voltage and resultant current is calculated and this is the impedance of the device under test [5].

The plotting of the real and imaginary parts of impedance $R(\omega)$, $X(\omega)$ on a complex plane in function of frequency gives the impedance spectrum of the device. From this diagram, the equivalent circuit parameters are calculated. In the case, the representation of $X(\omega)=f(R(\omega))$ in our case is called the Cole-Cole diagram [6-8]. which gives arcs centered below the real axis $R(\omega)$Thus, there is a depression angle θ, is appeared, between the real axis and the straight line defined by the origin of axis and the center of the circle containing the arc [6], that means, the relaxation time constant is dispersed.

2. Experimental Procedures

When conducted under different temperatures, this method provides many parameters of a solar cell, e.g., the temperature dependence of the shunt resistance and diode factor, the energy and concentration of the dominant recombination center, the lifetime of the charge carriers. The measuring apparatus works with a current source with a range of 0 to 100 mA (Keithly 2401). The temperature range is from approximately 298 K° to 353 K°. Input data were introduced into specially designed software that performs numerical calculations based on the double exponential model of a p-n junction formulated in dark by the following equation [9, 10]:

$$I = \frac{V - R_s I}{R_{sh}} + I_{o1}\left[\exp\left(\frac{V - R_s I}{V_T}\right) - 1\right] + I_{o2}\left[\exp\left(\frac{V - R_s I}{A V_T}\right) - 1\right] \quad (1)$$

Where:
I: Total cell current (A)
V: Cell voltage (V)
I_{01}: Diffusion reverse saturation current (A)
I_{02}: Recombination reverse saturation current (A)
R_s: Series resistance (Ω)
R_{sh}: Shunt resistance (Ω)
A: Ideality factor (1-2)
V_T: Voltage thermal ($V_T = KT/q$)
T: Cell working temperature in Kelvin degree (K)
q: Elementary charge = 1.602177×10^{-19} (C)
k: Boltzmann's constant = 1.380662×10^{-23} (J/K)

The AC parameters of silicon solar cell under dark condition by biasing the cell at the voltages 0.7 were measured at different temperatures (298, 333 and 353 K°), using the impedance spectroscopy technique which consists of a GAIN PHASE ANALYZER (Schlumberger-SI1253) which produces a frequency range varying from 1 mHz to 20 KHz and V_{dc} up 10 Volts, V_{ac} varies between 0 to 12 Volts, electrical furnace, its temperature varies between room temperature and 1500 t° programmable with 8 steps, personal computer and the MSiSC. We use an AC signal with amplitude equals to 0.7 V with the frequency ranging from 1 Hz to 20 KHz.

3. Results and discussion

3.1 DC measurements

I-V characteristics of the MSiSC under the dark conditions for different temperatures (298 - 353 K°) are shown in Fig. 1.

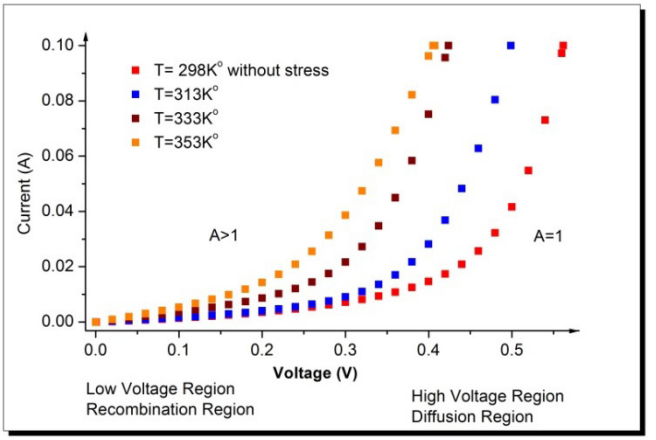

Fig. 1. I-V Characteristics of the MSiSC at temperate 298, 313, 333 and 350 K°.

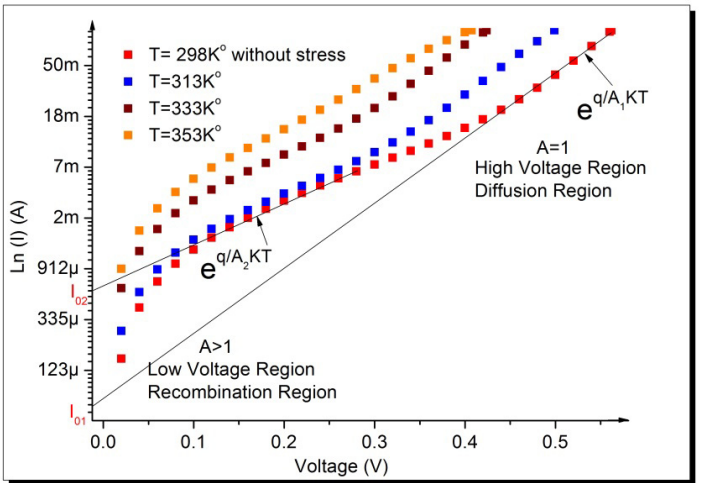

Fig. 2. Ln (I) as a function of applied voltage V at various temperatures.

From the figure1 we can draw the figure 2 representing as Ln(I)=f(V), shows the plotted graph of I-V characteristics is divided into two regions as mentioned in the previous two terms values A in the Eq.(1):
1) At low bias voltages or low current, the influence of shunt resistance, where generation and recombination of the electron-hole pairs in the junction depletion region dominants, the ideality factor value is larger than 1($A \rightarrow A_2$ and $I_0 \rightarrow I_{02}$), It is related with expression of the second exponential in Eq.(1). The interception of the curves gives Recombination reverse saturation current I_{02} (μA) (figure 3). The slope of the linear portion of the plot of Ln(I) vs. V gives also the factor A_2 (figure 4).

2) At high bias voltages, the first term in the expression of the total current that determines the diffusion compounds is dominated by the surfaces and the bulk regions, the ideality factor value is equal than 1($A \rightarrow A_1$ and $I_0 \rightarrow I_{01}$), so, by the curve fitting method, the Diffusion reverse saturation current and

the diffusion ideality factor can be extracted. The interception of the curves gives I_{01} (μA) (figure 3). The slope of the linear portion of the plot of Ln(I) vs. V gives also the factor A_1 (figure 4).

It is observed from figure 3, that the I_{01}, I_{02} in Si-solar cell increases exponentially with increasing T_F. From the variation of A as mentioned previously we suggest that the dark current is due to the generation-recombination of charge carriers within the depletion region.

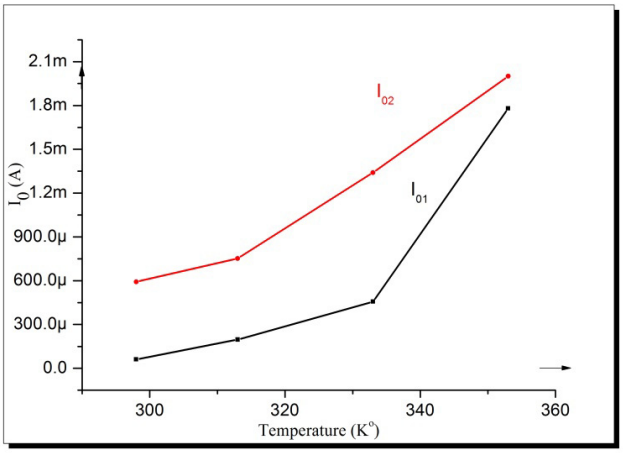

Fig. 3. The variation of I_{01} and I_{02} with T_F 298, 333 and 353 K°.

the ideality factor A as function of T_F, Our results show that, a small decrease in the ideality factor with increasing the temperatures may be caused by the increase of the saturation current I_o which is due to the modification of the current transport tunneling mechanism in the device. The decreasing diode ideality factors can thus be interpreted as a relative increase of recombination of carriers in the bulk of the material as compared to the recombination in the space-charge region these results are in agreement with others [11].

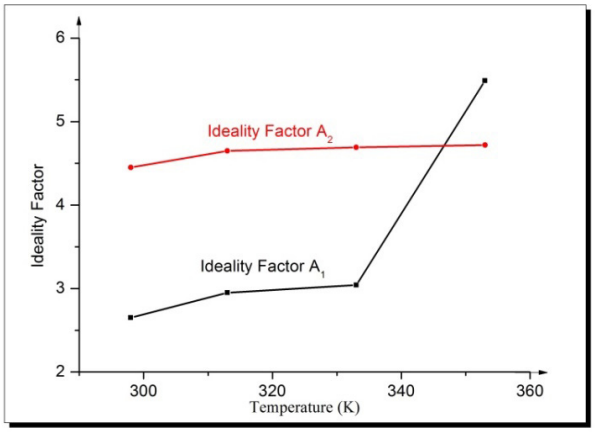

Fig. 4. The variation of the ideality factor A_1, A_2 with T_F 298, 333 and 353 K°.

From the slop of the ARREHENIUS plot defined by $Ln(I)=f(1/T)\,)|_{v=const}$ (figure 5), we have obtained the variation of barrier height Ψ (eV) with applied voltage.

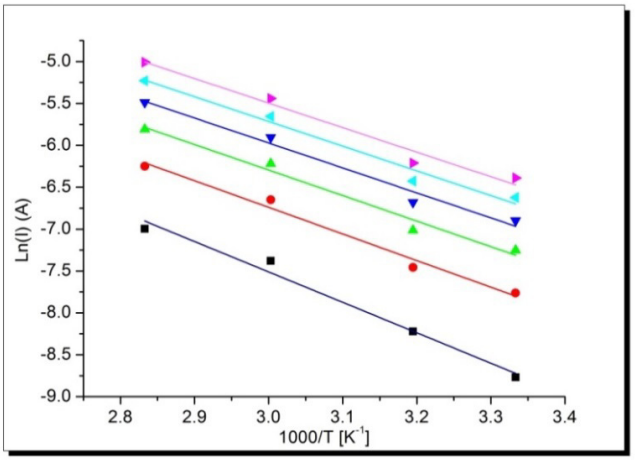

Fig. 5. ARREHENIUS diagrams defined by Ln(I) = f(1/T) at voltage constant.

The barrier height, Ψ, is about 0.392 eV in the region between 0.1 to 0.35 V. Above the threshold voltage V_s=0.33±0.02, the barrier height sharply decreases (Fig. 6).

The barrier height is given by [6]:

$$\Psi = \frac{q}{2\varepsilon_o \varepsilon_r} \frac{N_s^2}{N_d} \qquad (2)$$

Where:

ε_o: the vacuum dielectric constant, equal to 8.854×10^{-14} F/cm.

ε_r: the relative dielectric constant of silicon and 11.8.

N_s: density states.

N_d: donor density.

It is clear from the Eq.(2), the barrier height, Ψ, decreasing when applied voltage is increasing on the solar cell.is caused by:

- donor density N_d increasing.
- density states N_s is decreasing.

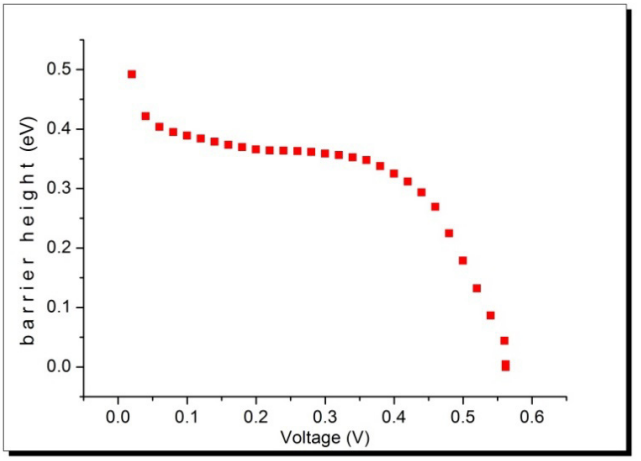

Fig. 6. The variation of the barrier height Ψ as a function of applied voltage.

3.2 AC measurements

The complex impedance spectroscopy (CIS) technique [12] was used to analyse the electrical response (i.e. transport properties) of the MSiSC in a wide range of frequency from 1 Hz to 20 KHz at T_F 298 K°, 333 K°, and 353 K°. Figure 7 show the variation of the real part R(ω) of impedance with frequency at various temperatures, respectively.

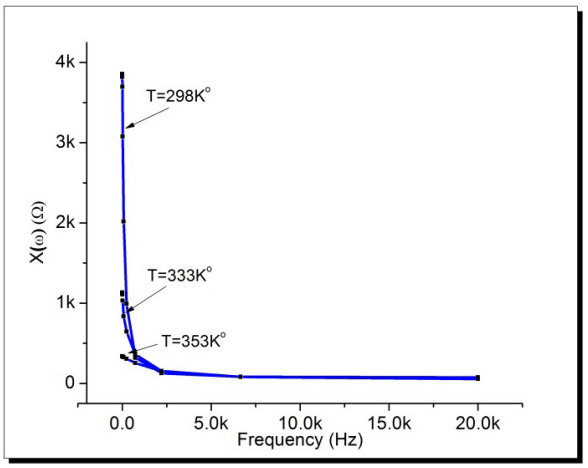

Fig. 7. the variation of the real part R(ω) of impedance with frequency at T_F 298, 333 and 353 K°.

It is observed that the magnitude of R(ω) decreases with the increase in both frequency as well as temperature indicating an increase in ac conductivity with the rise in temperature and frequency. The values of R(ω) for all temperatures merge above 2.25 KHz. This may be due to the release of space charges as a result of reduction in the barrier properties of material with the rise in temperature, and may be a responsible factor for the enhancement of ac conductivity of material with temperature at higher frequencies. Further, at low frequencies the value of R(ω) decreases with rise in temperature showing negative temperature coefficient of resistance (NTCR) type behaviour (like that of semiconductors).

Figure 8 show that the X(ω) values reach a maxima peak X(ω)max. The value of X(ω)max shifts to higher frequencies on increasing temperature. A typical peak broadening, which is slightly asymmetrical in nature, can be observed with the rise in temperature. The broadening of peaks (explicit plots of X(ω)) suggests that, there is a spread of relaxation time (i.e. the existence of a temperature dependent electrical relaxation phenomenon in the material [13]. The merging of X(ω) values in the high frequency region may possibly be an indication of the accumulation of space charge in the material. The peaks shift toward high frequency region with rise in temperature.

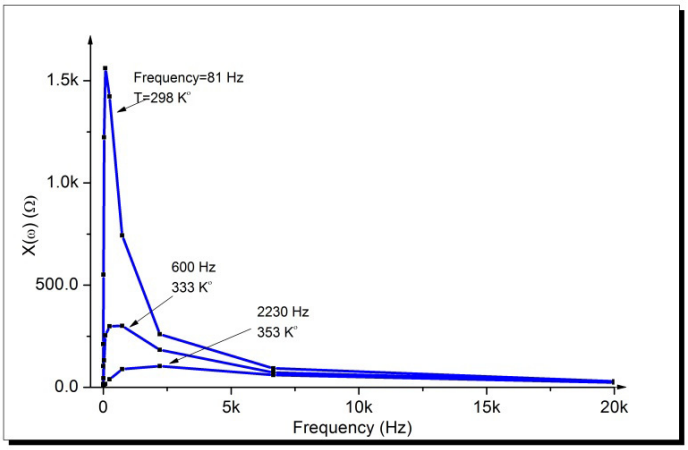

Fig. 8. the variation of the imaginary part X(ω) of impedance with frequency at T_F 298, 333 and 353 K°.

Figure 9 shows the relationship between the imaginary part X(ω) and the real part R(ω) of the complex impedance.

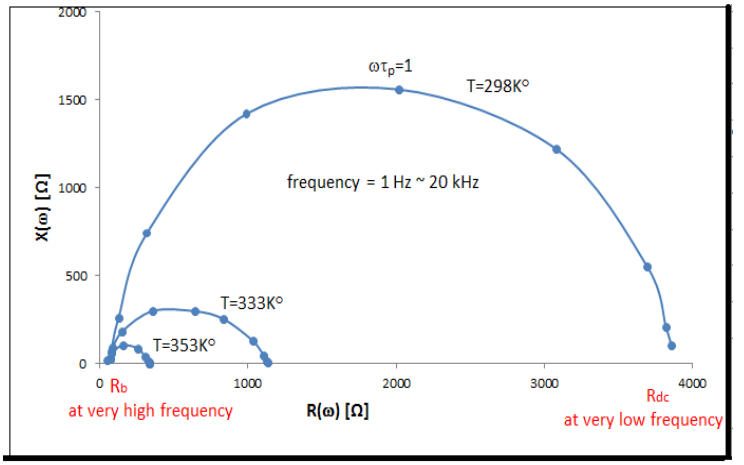

Fig. 9. Impedance spectra of the MSiSC at T_F 298, 333 and 353 K°.

The values of R(ω) and X(ω) are plotted as a function of temperature. We have obtained arcs of a semicircle which their centers lie below the real axis R(ω), corresponding to the appearance of the depression angle (θ≠0). It is noted that, θ, increases with temperature, which represents the heterogeneity factor β ($\beta = \theta/(\pi/2)$) and 0<β<1, it can be determined experimentally, and illustrated in (Fig. 9).

The centre of the semicircle arc shifts towards the origin on increasing temperature which indicates that the conductivity of the samples increases with increase in temperature. In this material, dipolar relaxation process occurs in the material since semicircular arcs are observed in the high-frequency zone. Single semicircular arcs observed in the complex plane at elevated temperatures reveal that the conduction in the material is predominant in grains rather than in grain boundaries.

From cole–cole diagrams (Fig. 9) we have obtained the values R_b and R_b+R_p from the graphic as the following table:

Table 2. Calculated values of R_b and R_b+R_p for different temperature

T_F (K°)	298	333	353
R_b+R_p (KΩ)	3.861	1.135	0.34
R_b (KΩ)	75E-3	70E-3	55E-3

The relaxation $\tau_p=RC$ is called the most probable relaxation time which can be also calculated from $\omega\tau_p=1$, $\omega=2\pi f$ at the summit of the arc. This is in good agreement with the Cole-Cole diagram. It is noted that, β, increases with T_F (Fig. 10). We propose that, the appearance of β is not zero, is due to of the presence of crystalline defects in the structure of the cell and/or heterogeneity in the process of deposition.

We observe also, that, the arc intersection point at the left-hand side of R(ω) axis gives the resistance corresponding to the bulk resistance R_b [$R(\omega)=R_b$ as $\omega\rightarrow\infty$], (i.e. at very high frequency). While, the arcs of semicircles, (on extension), intersect the right hand side of R(ω) axis at resistance values corresponding to the DC values R_{dc} [$R(\omega)=R_{dc}$ as $\omega\rightarrow0$], (i.e. at very low frequency). The resistance R_{dc} is equal to the leakage parallel resistance R_p as $\omega\rightarrow0$.

The centers of the arcs of semicircle obtained lie below the real axis R(ω), This indicates that the AC equivalent circuit of a solar cell is a resistance connected in parallel with the capacitance, Cp, with a single time constant.

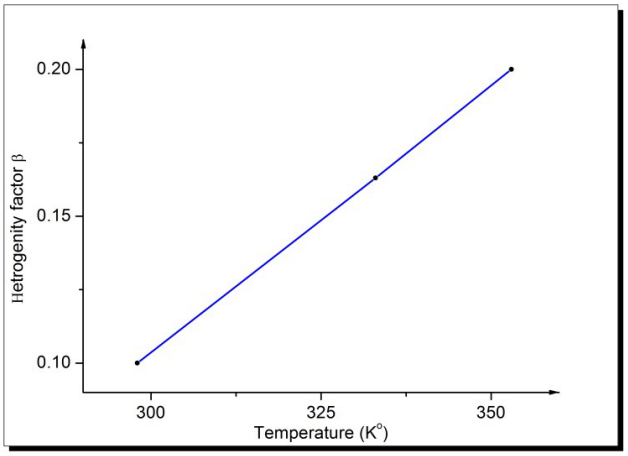

Fig. 10. The heterogeneity factor as a function of temperature.

Table 2. Calculated values of solar cell AC for different temperature

T_F (K°)	298	333	353
R(ω) (KΩ)	3.861	1.135	0.34
X(ω) (KΩ)	1.56	0.3	0.104
f (Hz)	81	600	2230
C_P (nF)	1260	885	687
τ_p (μS)	1970	265	71.4
R_P (KΩ)	1.56	0.3	0.104
β	0.1	0.163	0.2

The equivalent circuit for the solar cell is consists of a leakage resistance R_p connected in parallel with a capacitor C_p, both on the sequence with bulk resistance R_b as shown in figure 11.

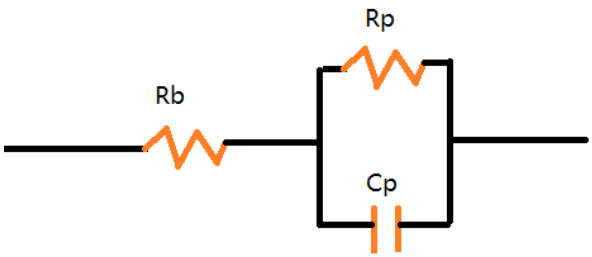

Fig 11. The equivalent circuit for the MSiSC.

The variation of capacitance with frequency for silicon solar measured under dark conditions at 0.7 V is shown in Fig. 12.

The table 2, shows that, the capacitance decreases with increase of frequency, indicating the presence of deep levels near junction interface [14]. The capacitance value decreases from 33.4 to 19 nF corresponding to the frequencies at summit of arcs (Fig.9) (f =81, 600 and 2230 Hz), for the irradiated sample.

To understand the decreasing of the capacitance Cp with the frequency, f, we can write: the flux of the current i(t) when the charge varies with the time by the following equation:

$$i(t) = \frac{dQ}{dt} \qquad (3)$$

Applying Laplace transform, we obtain the relationship:

$$C(s) = \frac{I(S)}{2\pi f V(s)} \qquad (4)$$

From this equation, it can be concluded that the capacitance C_p decreases with frequency. For the nature or the original of this capacitance, we suggest the following explanation: the interface states in equilibrium in the semiconductor do not contribute to the capacitance at sufficiently high frequencies because the charge at the interface states cannot follow the AC signal [15]. In this case, it is the space-charge capacitance only. At low frequencies, the contribution of the interface states to diode capacitance decreases with increasing frequency

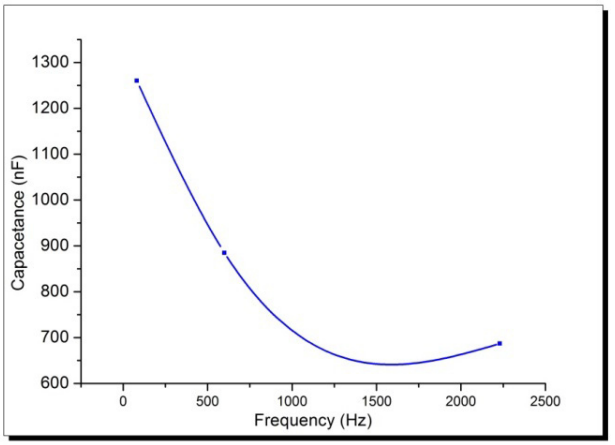

Fig. 12. Variation of capacitance with frequency at 0.7V for solar cell module.

To obtain the donor density N_d (cm^{-3}) and the surface state density, N_s (cm^{-2}), we obtain the activation energy E=0.102 eV from the slope of figure 13 which is the ARREHENIUS diagrams defined by Ln(c)=f(1/T). The summit position of X(ω) is exponentially activated with activation energy.

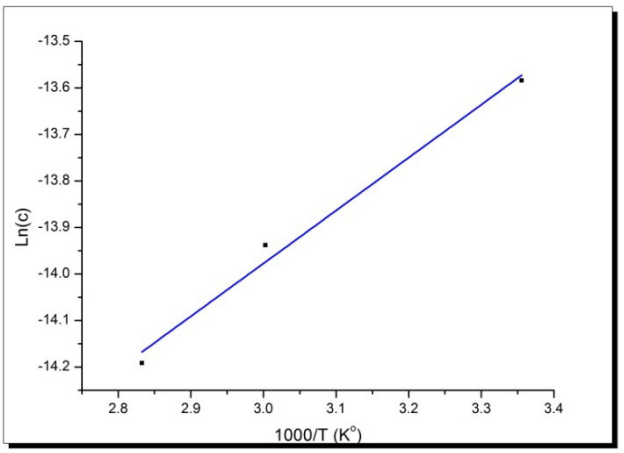

Fig. 13. ARREHENIUS diagrams defined by Ln(c) = f(1/T).

The donor density in the bulk is responsible for the transport mechanism, which can be calculated by the activation energy value E in the following relation:

$$N_d = N_o e^{-E/kT} \qquad (5)$$

Where: N_o the effective density of electrons (2.7×10^{18} cm^{-3} for silicon), K Boltzmann's constant ($8.626x10^{-5}$ (J/K)), and a density state N_s is given by:

$$N_s = \left(\frac{2\varepsilon_0\varepsilon_r N_d \Psi}{q}\right)^{1/2} \qquad (6)$$

Where: ε_o and ε_r are, respectively, the vacuum dielectric constant and the relative dielectric constant of silicon, equal to 8.854×10^{-14} F/cm and 11.8, respectively (Table 3).

Table 3. Variation of donor density N_d and density states N_s as a function of temperature

T_F (K°)	298	333	353	Average
N_d (cm^{-3})	5.22E+16	7.07E+16	9.18E+16	7.16E+16
N_s (cm^{-2})	2.64E+11	3.07E+11	3.49E+11	3.07E+11

We obtain the activation energy E=0.543 eV from the slope of figure 14 which is the ARREHENIUS diagrams defined by Ln(f)=f(1/T). The summit position of X(ω) is exponentially activated with activation energy. After that we obtain the donor density N_d (cm^{-3}) and the surface state density, N_s (cm^{-2}), (table 4).

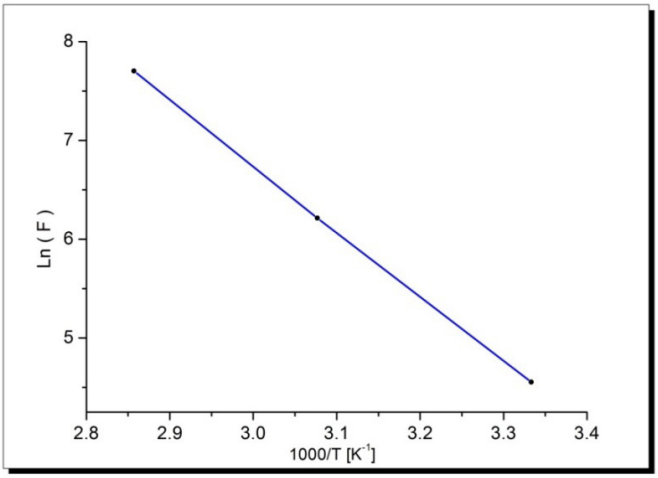

Fig. 14. ARREHENIUS diagrams defined by Ln(F) = f(1/T).

Table 4. Variation of donor density N_d and density states N_s as a function of temperature

T_F (K°)	298	333	353	Average
N_d (cm^{-3})	1.79E+9	1.65E+10	4.81E+10	2.21E+10
N_s (cm^{-2})	9.55E+7	2.90E+8	4.96E+8	2.94E+8

4. Conclusions

The I-V characteristics of solar cells at different temperatures were measured in the dark. We have obtained the barrier height Ψ (eV), ideal factor A, and the reverse saturation current I_0 (μA).

On using the AC impedance measurements, achieved on the solar cell in dark conditions, for different T_F (298 K° to 353 K°), we have determined some parameters, such as: heterogeneity factor β, DC resistance R_{dc}(Ω), the bulk resistance R_b(Ω), activation energy E (eV), donor density N_d (cm^{-3}), and density states N_s (cm^{-2}). It was concluded that, the leakage current that the density increases with temperature. The decreasing of the diode ideality factors can thus be interpreted as a relative increase of recombination of carriers in the bulk of the material as compared to the recombination in the space-charge region. The barrier height, Ψ, is (0.392 eV) in the voltage range varying from 0.1 to 0.35 V. Then, when the threshold voltage becomes above V_s=0.33±0.02, the barrier height sharply decreases.

Funds

This project has been funded by the Lebanese National Council for Scientific Research.

References

[1] Keithley Instruments, Inc., (2007), "Making I-V and C-V measurements on solar/ photovoltaic cells using the model 4200-SCS semiconductor characterization system", *Keithley Instruments*, Application note series number 2876, www.keithley.com, USA. Report downloaded Nov. 20, 2009.

[2] R. Anil Kumar, M.S. Suresh and J. Nagaraju, Ga As/Ge solar cell AC parameters at different temperatures. *Solar Energy Mater. Solar Cells*, **77** (2003), pp. 145–153.

[3] V. Schlosser and A. Ghitas. "Measurement of silicon solar cells ac parameters", *Proceedings of the Arab Regional Solar Energy Conference* (Manama, Bahrain, Nov 2006).

[4] R. Anil Kumar, M.S. Suresh and J. Nagaraju , Facility to measure solar cell AC parameters using an impedance spectroscopy technique. *Rev. Sci. Instrum.* **72(**8) (2001), pp. 3422–3426.

[5] Deshmukh, M.p. Nagaraju J, "Measurement of silicon and GaAs/Ge solar cell device parameters", *Solar Energy Materials&Solar Cell*, 89: 403-408 (2005).

[6] Khalaf Abdullah.; Bui Ai.; Loubierre A, "Low frequency and low temperature behavior of ZnO– based varistor by ac impedance measurements". *Journal of applied phys*, 69(7), 4046-4052 (1991).

[7] Watanabe, K., Taka, Y., Fujiwara, O. "Estimation of alcohol concentration of red wine based on Cole-Cole plot. IEEJ Trans". FM, (2009) 129 (5), 352-356.

[8] K.H.Cole and R.H.Cole, J.Chim. Phys. Vol. 9,pp 341-353 (1941).

[9] D. Lugo-Munoz, J. Muci, A. Ortiz-Conde, F.J. Garcia-Sanchez, M. de Souza, M and A. Pavanello, "An explicit multi-exponential model for semiconductor junction with series and shunt resistances", *Journal Microelectronics Reliability*, 51 2011) 2044-2048.

[10] Salame, C and Habchi. R., "Silicon MOSFET devices electrical parameters evolution at high temperatures", *Microelectronics International*, Vol. 25(2008), No. 1, pp. 21-24.

[11] A. Rao, S. Krishnan, G. Sajeev and K Siddappa, "Temperature and 8 MeV electron irradiation effects on GaAs solar cells", *Pramana -J. Phys*., Vol. 74(6) (2010), pp. 995-1008.

[12] MacDonald J R (1987) Impedance spectroscopy (New York: Wiley).

[13] Suman C K, Prasad K and Choudhary R N P (2005) Adv. Appl. Ceram. 104 294.

[14] K. Abdullah, A.Dewaydari, L. Kassas, "study of the behavior of some semiconductor material to be used in the direct conversion of solar energy to electrical energy", thesis (PhD), 2003.

[15] S M Sze, *Physics of semiconductor devices*, 2nd Edition (Wiley, New York, 1981) pp.807-809.